Korean J. Chem. Eng., **28**(4), 1078-1084 (2011)
DOI: 10.1007/s11814-010-0483-1

Introduction of heterogeneous NADH reoxidation pathways into *Torulopsis glabrata* significantly increases pyruvate production efficiency

Yi Qin*,, Clayton H Johnson***,****, Liming Liu*,***,†, and Jian Chen*,****

*State Key Laboratory of Food Science and Technology, Jiangnan University, 1800 Lihu Road, Wuxi, Jiangsu 214122, China
**School of Biotechnology and Key Laboratory of Industrial Biotechnology, Ministry of Education, Jiangnan University, 1800 Lihu Road, Wuxi, Jiangsu 214122, China
***D.W. Reynolds Department of Geriatrics (VAMC151/LR), University of Arkansas for Medical Sciences, 4300 W 7th St., Little Rock, Arkansas 72205, USA
****Biology Department, University of Arkansas at Pine Bluff, Pine Bluff, Arkansas 71601, USA
(*Received 10 June 2010 • accepted 15 November 2010*)

Abstract−The aim of this study was to increase pyruvate production efficiency in a multi-vitamin auxotrophic yeast, *Torulopsis glabrata*. This was achieved by decreasing intracellular NADH content through the introduction of two different NADH reoxidation pathways: one in the cytoplasm and the other in mitochondria. A *nox* (encoding a cytoplasmic H_2O-forming NADH oxidase) and an *AOX1* (encoding a mitochondrial alternative oxidase) were successfully expressed heterologously in *T. glabrata*, resulting in a decrease in the NADH and ATP contents of 55% and 26%, (in *T. glabrata* NOX) and 45% and 47% (in *T. glabrata* AOX), respectively. The decreases in nucleotide concentrations led to increases in the glucose consumption rate, the pyruvate yield and pyruvate productivity of 27%, 15% and 22% (in *T. glabrata* NOX) and 38%, 21%, and 29% (in *T. glabrata* AOX), respectively, compared with the corresponding values of the control. We conclude that this method provides an alternative way to enhance the production efficiency of NADH-related metabolites.

Key words: NADH, *Torulopsis glabrata*, Pyruvate, H_2O-forming NADH Oxidase, Alternative Oxidase

INTRODUCTION

Pyruvate is widely used as a nutraceutical in the pharmaceutical and agrochemical fields and, recently, as the key metabolic precursor to the second-generation biofuels isobutanol and 3-methyl-1-butanol [1]. *Torulopsis glabrata* is the only microorganism used in commercial fermentation to produce pyruvate [2]. To decrease pyruvate production costs, it is necessary to enhance production efficiency by improving pyruvate production, yield or productivity (namely, the pyruvate production rate). Among these approaches, improving pyruvate productivity via metabolic engineering or biochemical strategies seems potentially promising. As the pyruvate moiety resides biochemically at the end of the glycolysis pathway, pyruvate productivity mainly depends on the glycolytic flux. Therefore, an efficient and easy way to improve pyruvate productivity would seem to be to increase the carbon flux through the glycolytic pathway.

Carbon flux through glycolysis is exquisitely regulated by the intracellular NAD^+, NADH and ATP content [3-6]. In particular, NADH and NAD^+ play an important role in glucose catabolism through regulation of both the expression and activities of various glycolytic enzymes [7]. During glycolysis, the simultaneous conversion, in equivalent amounts, of NAD^+ to its reduced form (NADH) occurs. To increase carbon flux through the glycolytic pathway, therefore, it is crucial to supply enough NAD^+ to sustain glycolysis [8]. Hence, NADH produced from NAD^+-related metabolic pathways in the cytoplasm needs to be fully oxidized to NAD^+ via the oxidative phosphorylation pathway, external mitochondrial membrane-bound NADH dehydrogenase, glycerol-3-phosphate dehydrogenase and/or alcohol dehydrogenase [7]. However, when NADH reoxidation occurs in the cytoplasm, it will lead to carbon flux being channeled into other metabolic pathways. On the other hand, NADH is also generated in the mitochondria by the tricarboxylic acid (TCA) cycle. Since NADH/NAD^+ cannot traverse the mitochondrial membrane [9], mitochondrial NADH is oxidized mainly via the oxidative phosphorylation pathway, coupled with high ATP production. Thus, the redistribution of cytoplasmic carbon flux results in a decline in the pyruvate yield of *T. glabrata*. Moreover, the high ATP concentration in *T. glabrata* could cause allosteric inhibition on the glycolytic pathway, which would eventually also lead to a reduction in pyruvate productivity. Therefore, the ideal way to improve pyruvate production would be to design a way for the excessive NADH to be fully consumed, together with little or no ATP production and without any carbon flux redistribution. Our previous studies have proven that decreasing the ATP levels by disruption of the mitochondrial electron transport chain [10] or by over-expression of an F_0F_1-ATPase inhibitor *INH1* in *T. glabrata* [11] is an effective way to increase glycolytic flux and pyruvate production. However, such strategies are one-sided because they only consider reducing ATP production, without considering the physiological effect of NADH consumption.

According to the KEGG database (updated on April 6, 2010), NADH is involved in 433 enzymatic and 740 metabolic reactions

†To whom correspondence should be addressed.
E-mail: mingll@jiangnan.edu.cn

[12]. Most of those reactions are directly related to the redistribution of carbon flux. However, some reactions catalyzed by water-forming NADH oxidase (EC 1.6.99.3) [13] in the cytoplasm and alternative oxidase [14] in mitochondria only involve oxygen consumption and water formation and decouple the use of NADH for respiratory ATP generation. These two different NADH reoxidation pathways potentially provide a great opportunity to manipulate NADH metabolism in the industrial strain in order to enhance target metabolite production [7,13-16]. It has been observed that over-expression of *nox* or *AOX1* in *S. cerevisiae* leads to a large decrease in the intracellular NADH/NAD^+ ratio and NADH and ATP concentrations [7,16].

In this study, we introduced two different NADH reoxidation pathways to enhance pyruvate productivity and pyruvate yield. These pathways include heterologous production of a H_2O-forming NADH oxidase from *Streptococcus pneumoniae* and an alternative oxidase from *Histoplasma capsulatum* in *T. glabrata*. The introduction of these NADH reoxidation pathways reduced NADH and ATP levels in *T. glabrata*, which led to higher pyruvate productivity and yield. In addition, we compared the different mechanisms between the two NADH reoxidation pathways for increasing pyruvate production efficiency.

MATERIALS AND METHODS

1. Yeast Strain Construction

Plasmids and strains in this study are listed in Table 1. The H_2O-forming NADH oxidase gene (*nox*) from *Streptococcus pneumoniae* was PCR-amplified with pTEF-nox as template [13] by using high fidelity DNA polymerase probes (Takara, Dalian, China). The primers contain a *Bam*HI site (underlined) in the coding strand primer, 5′-TACGGATCCATGAGTAAAATCGTTGTAGTCGGTGC-3′, and a *Sal*I site (underlined) in the complementary strand primer, 5′-ACGGGTCGACCTTATTTTTCAGCCGTAAGGGCAGCC-3′. After gel purification the 1.3-kb *nox* was digested with the appropriate restriction enzymes and gel-isolated. A high copy number plasmid pYX212 with *TPI* promoter was also digested with the appropriate restriction enzymes and was used to ligate the amplified gene fragments, resulting in pYX212-NOX construct. These two plasmids were transformed into *T. glabrata* Δ*ura3* [17], and the resulting strains designated *T. glabrata* CON and *T. glabrata*, *T. glabrata* AOX, respectively.

2. Media and Growth Conditions

Slant and seed culture media was comprised (per liter) of 20 g glucose, 10 g peptone (Biochemical grade, Sino-American Biotechnology Co., Shanghai, China), 1.0 g KH_2PO_4 and 0.5 g $MgSO_4 \cdot 7H_2O$ for the liquid culture medium with 20 g agar added for the slant medium. The fermentation medium was comprised (per liter) of 100 g glucose, 7 g NH_4Cl, 5 g KH_2PO_4, 0.8 g $MgSO_4 \cdot 7H_2O$, 6 g acetate sodium, 4 mg nicotinic acid, 15 mg thiamine-HCl, 100 mg pyridoxine-HCl, 10 mg biotin and 50 mg riboflavin. Media were titrated to pH 5.0 with sterile $CaCO_3$. All vitamin additives were filter-sterilized prior to use.

The seed culture inoculated from a slant was cultivated in a 500-mL flask containing 50 mL seed culture medium on a reciprocal shaker for 24 h. Fermentation was carried out in a 3-L jar fermentor (Biotron, Biotron Inc., Korea) with 1.5 L of fermentation medium. The size of the inoculum was 10% (v/v). The pH of the fermentor cultures was automatically maintained at 5.0 by addition of an 8 M NaOH solution. The agitation speed and aeration rate were controlled at 300 rev/min and 4 vvm (volume of air per volume of broth per minute), respectively. All experiments were done in triplicate.

3. Analytical Methods

Cell concentration was determined from the optical density (Biospec-1601, Kyoto, Japan) at 660 nm after proper dilution and converted to dry cell weight (DCW) according to predetermined calibration ($OD_{660\,nm}$: DCW (g/L)=1 : 0.23) [18]. Glucose, pyruvate, α-ketoglutarate, glycerol and ethanol contents were determined by HPLC with an HPX-87H Aminex column (BioRad, CA, USA), eluted with 5 mM H_2SO_4 for separation at a flow rate of 0.6 mL/min and 65 °C, as described previously [20].

4. Quantitation of Intracellular NADH, NAD^+ and ATP

Intracellular NADH and NAD^+ were extracted from 10-mL cell aliquots after rapidly quenching metabolism by plunging the cells into 40 mL methanol prechilled for 4 h in a dry ice-ethanol bath. Chilled cells were centrifuged at 4,000 ×*g* and −20 °C for 1 min and immediately resuspended in 0.2 M HCl (to extract NAD^+) or 0.2 M NaOH (to extract NADH), and the nucleotides were extracted by boiling. A cycling assay was used to determine their concentrations [21,22], and ATP concentrations were determined after extraction as described previously [23].

5. Assay of Intracellular Enzymes

Cells from duplicate mid-log phase cultures (OD_{660nm}=6-8) were harvested and extracts were prepared from the pellets with a mag-

Table 1. Strains and vectors used in this study

Strain/Vector	Genotype/Description	Source
Strain		
T. glabrata CCTCC M202019	A multi-vitamin auxotroph strain	[18]
T. glabrata Δ*ura3*	A Δ*ura3* strain derived from *T. glabrata* CCTCC M202019	[17]
T. glabrata CON	*T. glabrata* Δ*ura3*/pYX212	This study
T. glabrata NOX	*T. glabrata* Δ*ura3*/pYX212-NOX	This study
T. glabrata AOX	*T. glabrata* Δ*ura3*/pYX212-AOX	[19]
Vector		
pYX212	2μ, TPI promoter's AMP^R	
pYX212-NOX	pYX212 with *nox* from pTEF-nox	This study
pTEF-nox	Containing H_2O-forming NADH oxidase gene *nox* from *S. pneumoniae*	[13]

netic stirrer (ACX 400 sonicator, 20 kHz, Sonic and Materials Inc., Newton, MA). Enzymes were assayed using the published procedures for total NADH oxidase [7], NADH-dependent glycerol-3-phosphate dehydrogenase (G3PDH) [24], NADH-dependent alcohol dehydrogenase (ADH) [25], NAD-dependent isocitrate dehydrogenase (ICDH) [26], glyceraldehyde-3-phosphate dehydrogenase (GAPDH), hexose kinase (HXK), phosphofructokinase (PFK), and pyruvate kinase (PYK) [23]. In all cases, 1 unit of enzyme activity was defined as the quantity of enzyme required to catalyze the conversion of 1 μmol substrate per minute under given assay conditions. The activity of alternative oxidase was assayed according to the method of Johnson et al. [14]. Protein concentrations were measured by the Lowry method with bovine serum albumin as the standard.

6. Gene Expression Analysis by Quantitative RT-PCR (qPCR)

The mRNA was extracted from yeast cells by the hot phenol method [27]. The transcriptional levels of the genes were determined via a quantitative PCR strategy (qPCR) with SYBR Premix Ex Taq™ II (Takara, Dalian, China) using *ACT1* as an internal standard [28]. The PCR reactions were performed on a Bio-Rad iCycler and analyzed with iCycler IQ software Version 3.0a (Bio-Rad, Hercules, CA, USA). At least three experiments were run for each condition in our study. The transcriptional level was analyzed by using the $2_T^{-\Delta\Delta C}$ method [29].

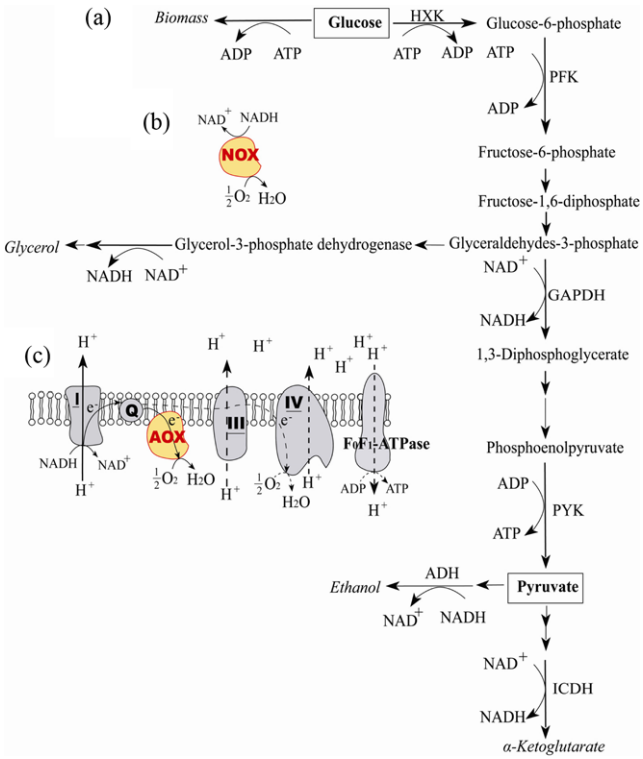

Fig. 1. Schematic of the pathways and key enzymatic reactions in the production of pyruvate and glycolytic by-products (a) in *T. glabrata*, including the new NADH-dependent water-forming NADH oxidase (b) and alternative oxidase (c). The by-products are indicated by italics in the figure. ADH: alcohol dehydrogenase; AOX: alternative oxidase; GAPDH: glyceraldehyde-3-phosphate dehydrogenase; G3PDH: glycerol-3-phosphate dehydrogenase; ICDH: NAD-dependent isocitrate dehydrogenase; NOX: water-forming NADH oxidase.

RESULTS AND DISCUSSION

1. Effects of the Introduction of NADH Reoxidation Pathways on Intracellular Nucleotide Concentrations

The *nox* gene from *S. pneumoniae* (encoding H_2O-forming NADH oxidase) [13] and *AOX1* (encoding alternative oxidase) from *H. capsulatum* [14] were overexpressed in *T. glabrata* Δ*ura3* and created the mutant strains *T. glabrata* NOX and *T. glabrata* AOX, respectively. The specific NADH oxidase activity in strain *T. glabrata* NOX is 4.65 U/mg protein, whereas it is only 1.33 U/mg protein in the control strain (*T. glabrata* CON) (Fig. 2(a)). Functional expression of alternative oxidase in the *T. glabrata* AOX strain was demon-

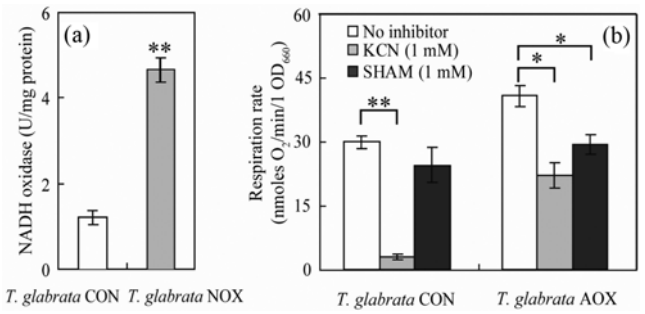

Fig. 2. Functional expression of NADH oxidase (a) and alternative oxidase (b) in *T. glabrata*. Values are expressed as mean ±SD (n=3). Significant difference from control: **, $P<0.01$; *, $P<0.05$.

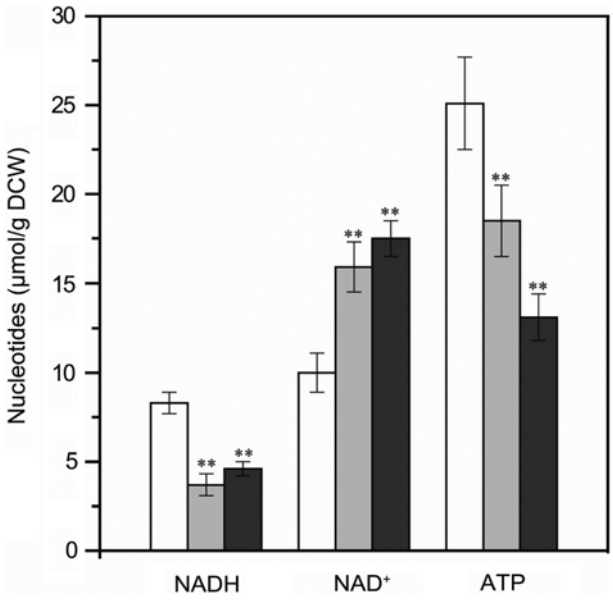

Fig. 3. The variances of intracellular NADH, NAD^+ and ATP levels. *T. glabrata* CON (white column), *T. glabrata* NOX (gray column) and *T. glabrata* AOX (black column). Each value corresponds to the mean±SD for three independent determinations. Statistically significant differences compared with *T. glabrata* CON were determined by Student's *t* test with significance as follows: *, $P<0.05$; and **, $P<0.01$.

strated by measurements of cyanide-insensitive oxygen consumption activity that was fully inhibited by salicyl hydroxamic acid, a specific inhibitor of alternative oxidase; however, no activity was detected in *T. glabrata* CON [19] (Fig. 2(b)).

The effects of H_2O-forming NADH oxidase or alternative oxidase expression on *T. glabrata* intracellular concentrations of NADH, NAD^+, and ATP were studied during aerobic mid-log batch cultivations of *T. glabrata* NOX, *T. glabrata* AOX and *T. glabrata* CON strains (Fig. 3). The overproduction of *nox* in *T. glabrata* NOX reduced the intracellular NADH content by 55.4% and the ATP concentration by 26.3% (from 25.1 μmol/g DCW to 18.5 μmol/g DCW), compared with the corresponding values for *T. glabrata* CON. Similarly, the intracellular NADH and ATP content was reduced by 44.6% and 47.8%, respectively, with the over-expression of *AOX1* in the *T. glabrata* AOX strain. The reasons for the decrease in the intracellular nucleotide concentration were: (1) the H_2O-forming NADH oxidase directly converted cytoplasmic NADH to NAD^+, decoupling the use of NADH for respiratory energy generation [16]; and (2) the mitochondrial alternative oxidase acted as a branched electron transport chain to reduce oxygen to H_2O [14,30,31].

2. Effects of the Introduction of NADH Reoxidation Pathways on Pyruvate Fermentation

As shown in Fig. 4, the heterologous NADH reoxidation pathways exerted a significant impact on the carbon flux distribution in *T. glabrata*. The accumulation of pyruvate was enhanced and the final fermentative pyruvate volumetric productivities of *T. glabrata* NOX and *T. glabrata* AOX were 12.5% and 19.0% higher, respectively, than that of the control strain (*T. glabrata* CON). Correspondingly, the pyruvate yield on glucose and pyruvate productivity also increased by 15.1% and 22.3% (*T. glabrata* NOX) and 20.9% and 29.3% (*T. glabrata* AOX), respectively (Table 2).

The improvement in pyruvate yield may be due to a reduction in the synthesis of by-products. The biomasses of the engineered strains were lower by 16.2% (*T. glabrata* NOX) and 22.2% (*T. glabrata* AOX) compared to that of the control (*T. glabrata* CON) (Fig. 4(a)). This is because of increased energy dissipation in the engi-

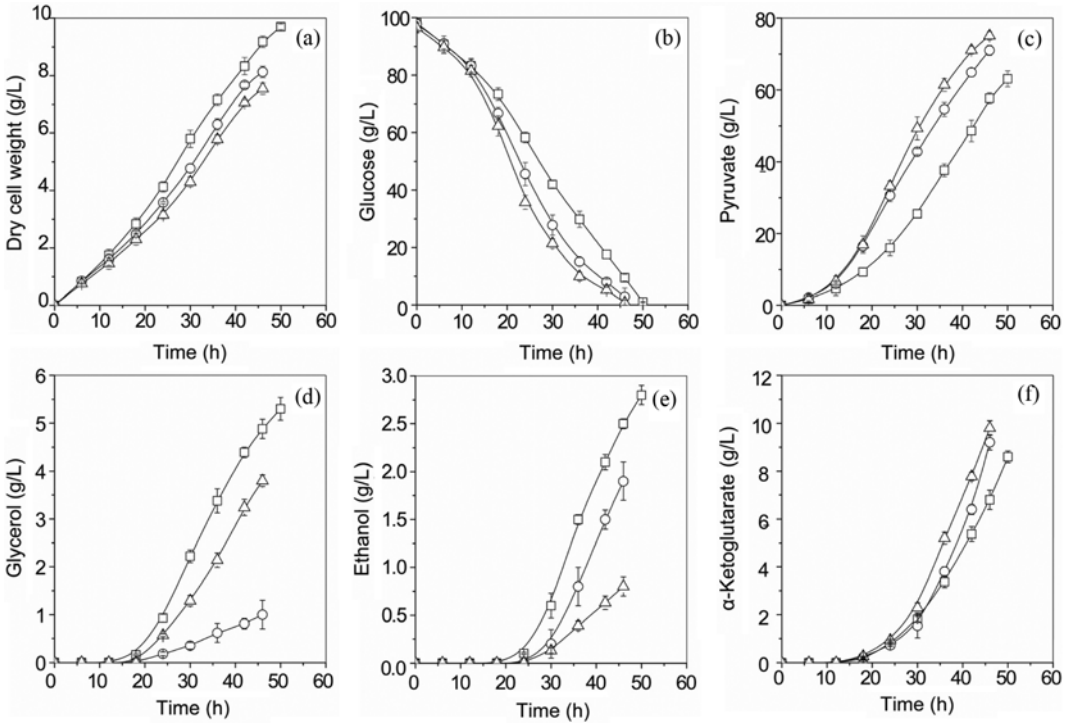

Fig. 4. Concentrations of biomass and by-products present in aerobic batch culture of *T. glabrata* CON (□), *T. glabrata* NOX (○) and *T. glabrata* AOX (△). Data represent the average and SD from three independent cultivations.

Table 2. Parameters of *T. glabrata* in batch cultures with different perturbations of NADH metabolism

Strain	q_s (g/g DCW h^{-1})†	Yield from glucose (g/g)¶					Pyruvate productivity (g/h)
		Pyruvate	Biomass	α-Ketoglutarate	Glycerol	Ethanol	
T. glabrata CON	0.20±0.01	0.65±0.03	0.10±0.01	0.13±0.01	0.08±0.01	0.03±0.00	1.26±0.06
T. glabrata NOX	0.25±0.01**	0.75±0.02**	0.09±0.01	0.14±0.02	0.02±0.00**	0.02±0.00	1.54±0.04**
T. glabrata AOX	0.28±0.02**	0.79±0.02**	0.08±0.00*	0.15±0.01	0.06±0.01	0.01±0.00**	1.63±0.04**

†The specific glucose consumption rate

¶All values were calculated from measurements made on batch cultures at the end of fermentation

Each value corresponds to the mean±SD for three independent determinations. Statistically significant differences compared with *T. glabrata* CON were determined by Student's *t* test with significance as follows: *, $P<0.05$; **, $P<0.01$

Table 3. Specific activities of the NAD(H)-dependent dehydrogenases and the key glycolytic enzymes of *T. glabrata* at the mid-log growth phase

Enzyme	Specific activities (U/mg protein)			Gene	The transcription level (-fold change)	
	T. glabrata CON	*T. glabrata* NOX	*T. glabrata* AOX		*T. glabrata* NOX	*T. glabrata* AOX
GAPDH [EC:1.2.1.12]	2.25±0.04	2.30±0.02	2.62±0.05	*TDH1*	+1.6±0.1	+1.1±0.1
				TDH2	+1.8±0.2	+1.3±0.0
G3PDH [EC:1.1.1.8]	0.40±0.01	0.10±0.01**	0.32±0.03	*GPD1*	−2.7±0.6	+1.1±0.0
				GPD2	−3.8±0.3	−1.6±0.0
ADH [EC:1.1.1.1]	0.04±0.01	0.02±0.01*	0.01±0.01**	*ADH1*	−2.0±0.2	−3.2±0.3
				ADH2	−1.1±0.0	−13.4±0.5
				ADH3	−1.8±0.3	−1.2±0.1
ICDH [EC:1.1.1.42]	5.58±0.02	6.01±0.02	5.85±0.02	*IDH1*	+1.2±0.2	+2.6±0.3
				IDH2	+1.5±0.1	+1.3±0.0
				IDH3	−1.4±0.0	+1.2±0.0
HXK [EC:2.7.1.1]	1.42±0.02	2.54±0.01**	2.11±0.01**	*HXK1*	+1.5±0.1	+1.6±0.1
				HXK2	+1.7±0.1	+5.5±0.3
				HXK3	+2.8±0.3	+1.2±0.0
PFK [EC:2.7.1.11]	1.43±0.20	3.81±0.03**	4.02±0.15**	*PFK1*	+8.8±0.5	+13.1±0.4
				PFK2	+10.8±0.6	+20.6±0.6
				PFK3	+2.3±0.3	+5.8±0.3
PYK [EC:2.7.1.40]	0.32±0.03	0.46±0.02*	0.61±0.01**	*PYK1*	+1.7±0.1	+1.3±0.1
				PYK2	+2.4±0.3	+7.9±0.3

Up-regulated genes are indicated by (+) and down-regulated ones are indicated by (–). ADH: alcohol dehydrogenase; GAPDH: glyceraldehyde-3-phosphate dehydrogenase; G3PDH: glycerol-3-phosphate dehydrogenase; HXK: hexokinase; ICDH: NAD-dependent isocitrate dehydrogenase; PFK: phosphofructokinase; PYK: pyruvate kinase. The values are averages of the results for three experimental samples and the error bars represent the standard deviation (n=3). Statistically significant differences compared with *T. glabrata* CON were determined by Student's *t* test with significance as follows: *, $P<0.05$; and **, $P<0.01$

neered strains [7]. Compared with the corresponding values for *T. glabrata* CON, the glycerol and ethanol yields on glucose were decreased by 75.0% and 33.3% in *T. glabrata* NOX and 25.0% and 66.7% in *T. glabrata* AOX, respectively. H_2O-forming NADH oxidase was found to have a profound impact on glycerol generation, whereas alternative oxidase exhibited a strong role in ethanol synthesis. Both moieties have various means of controlling the carbon flux distribution at the pyruvate node. A similar effect of alternative oxidase on ethanol production was also observed for the *S. cerevisiae* case [7]. Although Goutham's results suggested that the overexpression of alternative oxidase increased the TCA cycle capacity in *S. cerevisiae* and permitted more carbon flux from glycolysis to enter the TCA cycle [7], in our study the concentrations of key TCA cycle metabolites, specific for α-ketoglutarate, remained unchanged. This result strongly suggested that no more carbon flux could channel into the TCA cycle in *T. glabrata*. The reason is that *T. glabrata* is a thiamine-auxotrophic yeast, and the activities of the pyruvate dehydrogenase complex and α-ketoglutarate dehydrogenase in *T. glabrata* are determined by the sub-optimal thiamin content in the fermentation medium [32].

3. Effects of the Introduction of NADH Reoxidation Pathways on Key Enzymatic Activities and Transcript Levels

To illustrate the impact of heterologous NADH reoxidation pathways on the glycolytic pathway and the carbon flux distribution (Table 2), the activities of the NAD(H)-dependent dehydrogenases (G3PDH, ADH and ICDH) and the key glycolytic enzymes (HXK, PFK and PYK) were determined for *T. glabrata* CON, *T. glabrata* NOX and *T. glabrata* AOX (Table 3). As shown in Table 3, the G3PDH and ADH activities were lower by 75.0% and 50.0% (*T. glabrata* NOX) and 20.0% and 75.0% (*T. glabrata* AOX), respectively, compared to the corresponding values for *T. glabrata* CON. This result explains why the glycerol and ethanol yields on glucose were reduced with the lower intracellular NADH and ATP content. When the G3PDH and ADH activities and the glycerol and ethanol yields on glucose in *T. glabrata* NOX and *T. glabrata* AOX were compared with each other, we found that the lower the enzymatic activity, the lower the concentration of enzyme specific product. However, the GAPDH and ICDH activities were not significantly affected by the changes in intracellular NADH content (Table 3). The decreased availability of the nucleotide further increased the key glycolytic enzymatic activities, such as those of HXK, PFK and PYK. Compared with those of the control, the activities of HXK, PFK and PYK were higher by 78.9%, 166.4% and 43.8% (in *T. glabrata* NOX) and 48.6%, 181.1% and 90.6% (in *T. glabrata* AOX), respectively. Similar results were also observed in *S. cerevisiae*, where ATP has a strong negative effect on PFK and PYK activities [33].

Furthermore, the transcript levels of the encoding genes in the engineered strains and *T. glabrata* CON (at the mid-log growth phase, 30 h) were analyzed. As illustrated in Table 3, the transcript levels for the genes involved in the glycerol and ethanol synthesis path-

ways were significantly reduced. Over-expression of H_2O-forming NADH oxidase resulted in reductions in the transcript levels for *GPD1*, *GPD2* and *ADH1* of 2.7-fold, 3.8-fold and 2.0-fold, respectively, compared to those of the control, whereas over-expression of alternative oxidase had more pronounced effects on the genes encoding ADH, so that *ADH1* and *ADH2* transcription levels were decreased by 3.2-fold and 13.4-fold, respectively. Furthermore, the over-expression of H_2O-forming NADH oxidase and alternative oxidase both resulted in significant enhancements of the genes encoding key glycolytic enzymes, especially *PFK1* and *PFK2*.

The enhancement of the key glycolytic enzyme activities and transcript levels led to a higher carbon flux through glycolysis in *T. glabrata* NOX and *T. glabrata* AOX (Table 2). However, the physiological mechanisms for the higher glycolytic flux in *T. glabrata* NOX and *T. glabrata* AOX may be different. The heterologous production of *nox* provides an additional cytoplasmic NADH oxidation pathway in *T. glabrata* NOX, and this direct NADH consumption pathway continues to supply sufficient NAD^+ for glycolysis. However, the NADH/NAD^+ couple cannot be transported freely across the mitochondrial membrane in eukaryotic cells [34]. This means that even if the mitochondrial NADH were fully oxidized to NAD^+, the resulting NAD^+ could not be transported to the cytoplasm and could not be used for glycolysis. Therefore, the likely mechanism of the increased glycolytic flux in *T. glabrata* AOX is that the overexpression of alternative oxidase redirects the NADH oxidation pathway and consequently decreases the synthesis of ATP.

CONCLUSIONS

The pathway for pyruvate production from glucose via glycolysis is a cofactor-dependent pathway (Fig. 1), and the availability of nicotinaminde adenine dinucleotide (NADH and NAD^+) is the rate-limiting factor in the glycolytic pathway. To increase the carbon flux through glycolysis, and thus pyruvate production efficiency, it is crucial to have a constant supply of sufficient NAD^+. Hence, two different NADH reoxidation pathways, namely the H_2O-forming NADH oxidase cytoplasmic pathway and the alternative oxidase mitochondrial pathway, were heterologously expressed in the pyruvate producer *T. glabrata*. The introduction of the two different NADH reoxidation pathways resulted in decreases in NADH and ATP content. The decrease in nucleotide concentrations led to increases in the glucose consumption rate, the pyruvate yield and pyruvate productivity of 27%, 15% and 22% (in *T. glabrata* NOX) and 38%, 21%, and 29% (in *T. glabrata* AOX), respectively, compared to those of the control.

Improving NADH oxidation to NAD^+ and limiting ATP production, via heterologous H_2O-forming NADH oxidase and alternative oxidase, provided convenient means to sustain a high glycolytic rate, pyruvate production and pyruvate yield in *T. glabrata*. The introduction of two NADH oxidation pathways in *T. glabrata* provided a viable metabolic engineering strategy for increasing the production efficiency of fine chemicals in yeast.

ACKNOWLEDGEMENTS

This work was supported by the National Science Foundation for Distinguished Young Scholars (20625619), the National Natural Science Foundation of China (20706025), the Key Project of China National Programs for Fundamental Research and Development (2007CB714303) and the Foundation for the Author of National Excellent Doctoral Dissertation of China (200962).

NOMENCLATURE

ADH : alcohol dehydrogenase
AOX1 : alternative oxidase gene
AOX : alternative oxidase
ATP : adenosine triphosphate
DCW : dry cell weight
G3PDH : glycerol-3-phosphate dehydrogenase
GAPDH : glyceraldehyde-3-phosphate dehydrogenase
HXK : hexokinase
ICDH : NAD^+-dependent isocitrate dehydrogenase
PFK : phosphofructokinase
PYK : pyruvate kinase
q_s : specific glucose consumption rate
NADH : nicotinamide adenine dinucleotide
nox : H_2O-forming NADH oxidase gene
NOX : H_2O-forming NADH oxidase

REFERENCES

1. Y. H. Zhu, M. A. Eiteman, R. Altman and E. Altman, *Appl. Environ. Microbiol.*, **74**, 6649 (2008).
2. Y. Li, J. Chen and S. Y. Lun, *Appl. Biochem. Biotechnol.*, **57**, 451 (2001).
3. C. Larsson, A. Nilsson, A. Blomberg and L. Gustafsson, *J. Bacteriol.*, **179**, 7243 (1997).
4. T. B. Causey, K. T. Shanmugam, L. P. Yomano and L. O. Ingram, *Proc. Natl. Acad. Sci. USA*, **101**, 2235 (2004).
5. L. Pritchard and D. B. Kell, *Eur. J. Biochem.*, **269**, 3894 (2002).
6. G. S. Chuang and M. S. Chiou, *Korean J. Chem. Eng.*, **23**, 419 (2006).
7. G. N. Vemuri, M. A. Eiteman, J. E. McEwen, L. Olsson and J. Nielsen, *Proc. Natl. Acad. Sci. USA*, **104**, 2402 (2007).
8. K. G. Alberti, *J. Clin. Pathol. Suppl. (R Coll Pathol)*, **11**, 14 (1977).
9. M. Rigoulet, H. Aguilaniu, N. Averet, O. Bunoust, N. Camougrand, X. Grandier-Vazeille, C. Larsson, I. L. Pahlman, S. Manon and L. Gustafsson, *Mol. Cell. Biochem.*, **256-257**, 73 (2004).
10. L. M. Liu, Y. Li, H. Li and J. Chen, *FEMS Yeast Res.*, **6**, 1117 (2006).
11. J. W. Zhou, L. X. Huang, L. M. Liu and J. Chen, *J. Biotechnol.*, **144**, 120 (2009).
12. M. Kanehisa, S. Goto, M. Hattori, K. F. Aoki-Kinoshita, M. Itoh, S. Kawashima, T. Katayama, M. Araki and M. Hirakawa, *Nucleic. Acid. Res.*, **34**, D354 (2006).
13. J. Hou, N. F. Lages, M. Oldiges and G. N. Vemuri, *Metab. Eng.*, **11**, 253 (2009).
14. C. H. Johnson, J. T. Prigge, A. D. Warren and J. E. McEwen, *Yeast*, **20**, 381 (2003).
15. S. Guerrero-Castillo, M. Vazquez-Acevedo, D. Gonzalez-Halphen and S. Uribe-Carvajal, *Biochim. Biophys. Acta*, **1787**, 75 (2009).
16. S. Heux, R. Cachon and S. Dequin, *Metab. Eng.*, **8**, 303 (2006).
17. J. W. Zhou, Z. Dong, L. Liu, G. Du and J. Chen, *J. Microbiol. Methods*, **76**, 70 (2009).

18. L. M. Liu, Y. Li, H. Z. Li and J. Chen, *Lett. Appl. Microbiol.*, **39**, 199 (2004).
19. Y. Qin, Z. Y. Dong, J. W. Zhou, L. M. Liu and J. Chen, *Wei Sheng Wu Xue Bao*, **49**, 1483 (2009).
20. M. Moreira dos Santos, V. Raghevendran, P. Kotter, L. Olsson and J. Nielsen, *Metab. Eng.*, **6**, 352 (2004).
21. C. Bernofsky and M. Swan, *Anal. Biochem.*, **53**, 452 (1973).
22. M. R. Leonardo, P. R. Cunningham and D. P. Clark, *J. Bacteriol.*, **175**, 870 (1993).
23. L. M. Liu, Y. Li, Z. Shi, G. Du and J. Chen, *J. Biotechnol.*, **126**, 173 (2006).
24. A. Valadi, K. Granath, L. Gustafsson and L. Adler, *J. Biol. Chem.*, **279**, 39677 (2004).
25. E. Postma, C. Verduyn, W. A. Scheffers and J. P. Van Dijken, *Appl. Environ. Microbiol.*, **55**, 468 (1989).
26. A. P. Lin and L. McAlister-Henn, *J. Biol. Chem.*, **277**, 22475 (2002).
27. R. Klassen, J. Fricke, A. Pfeiffer and F. Meinhardt, *Biotechnol. Lett.*, **30**, 1041 (2008).
28. H. Muller, C. Hennequin, J. Gallaud, B. Dujon and C. Fairhead, *Eukaryot. Cell.*, **7**, 848 (2008).
29. K. J. Livak and T. D. Schmittgen, *Methods*, **25**, 402 (2001).
30. A. L. Moore and J. N. Siedow, *Biochim. Biophys. Acta*, **1059**, 121 (1991).
31. D. A. Berthold, N. Voevodskaya, P. Stenmark, A. Graslund and P. Nordlund, *J. Biol. Chem.*, **277**, 43608 (2002).
32. D. D. Zhang, N. Liang, Z. P. Shi, L. M. Liu, J. Chen and G. C. Du, *Biotechnol. Bioprocess. Eng.*, **14**, 134 (2009).
33. C. Larsson, I. L. Pahlman and L. Gustafsson, *Yeast*, **16**, 797 (2000).
34. G. von Jagow and M. Klingenberg, *Eur. J. Biochem.*, **12**, 583 (1970).